TURBULENT NATURAL CONVECTION FLOW AND HEAT TRANSFER IN AN INCLINED SQUARE ENCLOSURE***

Man-Heung Park* and Jae-Heon Lee**

(Received August 3, 1991)

Numerical analysis was performed for the two-dimensional turbulent natural convection in an inclined enclosure. The enclosure has two walls which one is heated and the other cooled, and has the other two walls of the linear temperature distributions. The inclined angle is equal to zero when the wall of linear temperature was horizontal and increases counter-clockwise. The mean continuity, mean momentum and mean energy equations have been obtained by using the conventional time-averaging procesure. The turbulent model has been applied a k-ε two equation model of turbulence similar to the one proposed by the Launder and Spalding. Numerical results were studied for a series of inclined angle, ranging from 0° to 60° and for a Grashof number range of $6\times10^6\sim10^8$. The average heat transfer rate on hot wall is shown maximum value at 30° regardless of Grashof number taken here. When $Gr\geq5\times10^7$ and $\theta\geq45°$, the flow region of whole enclosure became a significant turbulence.

Key Words: Tubulent Natural Convection, k-ε Model, SIMPLE Algorithm, Enclosure

NOMENCLATURE

C_1, C_2, C_3, C_μ	: Empirical turbulence model constants
G	: Production of turbulent kinetic energy by shear
g	: Acceleration of gravity
Gr	: Grashof number (Eq. 3d)
k	: Turbulent kinetic energy
L	: Width and height of enclosure
Nu	: Nusselt number (Eq. 14 and Eq. 15)
p	: Pressure
p'	: Effective pressure (Eq. 2)
Pr	: Prandtl number
S	: Source term
T	: Temperature
u,v	: Flow velocity
x,y	: Cartesian Coordinate
α	: Thermal diffusivity
β	: Coefficient of thermal expansion
Γ	: Exchange coefficient
Δ_1	: Dimension of the first node from the wall
ε	: Dissipation rate of tubulent kinetic energy
θ	: Inclined angle
κ	: Von Karman's constant
l	: Characteristic length scale of turbulence
μ	: Molecular viscosity
μ_t	: Turbulent viscosity
ν	: Kinematic viscosity
ρ	: Denisty
σ_k	: Prandtl-Schmidt number for the turbulent kinetic energy
σ_T	: Turbulent Prandtl number
σ_ε	: Prandtl-Schmidt number for the dissipation rate of turbulent kinetic energy
ϕ	: General dependent variable
	Superscripts
*	: Physical quantity
—	: Average value
	Subscripts
C	: Cold wall
eff	: Effective value
H	: Hot wall
L	: Wall of linear temperature
max	: Maximum value
o	: Reference quantity

*System Eng. Research Dept., Korea Power Engineering Company, Inc., P.O. Box 631, Yeoung-Dong, Seoul, Korea
**Department of Mechanical Engineering, Hanyang University, Seoul 133~791, Korea
***This paper was presented at the International Symposium on the Refined Flow Modeling and Turbulent Measurement, Iowa City, Iowa, U.S.A., 1985

1. INTRODUCTION

The buoyancy-driven flow in an enclosed cavity has many practical application. The above process include nuclear-reactor insulation, ventilation of rooms, solar-energy collection and crystal growth in liquids. There is an ever increasing amount of research on confined natural convection. Since Fraikin et al.(1980) applied the k-ε model proposed by Launder and Spalding to analyze the turbulent natural convection problem in a square enclosure, some investigations on turbulent natural convection in an enclosed space have been carried out. Markatos et al.(1984) presented numerical solution up to Rayleigh number of 10^{16} for a square enclosure. They reported that the range of core temperature decreased at first to the Rayleigh number of 10^8 and then increased again up to Rayleigh number of 10^{16}. In the above investigation, the Prandtl number of the test fluid was chosen similar to that of air. In addition, they looked on the flow region as turbulent one beyond the Rayleigh number of 10^6. Ozoe et al.(1985) examined numerically the turbulent natural

convection in a square enclosure filled with water. They considered that the flow region became turbulence beyond the Rayleigh number of 10^{10}. They also reported that the solution using turbulent Prandtl number of 4 and the constant C_1 of 1.296 in the ε equation showed fairly good agreement with their experimental data. Davidson(1990(a), 1990(b)) applied the modified form of a low Reynolds number k-ε turbulence model and the hybrid turbulence model (k-ε model+algebraic Reynolds stress (ASM) model) to analyze the turbulent natural convection problem in a tall two-dimensional cavity of 5 : 1 aspect ratio. Ideriah(1980) presented some numerical results with the k-ε model for mixed turbulent convection in a rectangular space. He applied the wall function proposed for the forced convection to predict turbulent quantities. For a horizontal circular cylinder, Farouk(1981) employed the k-ε model to obtain numerical solution of the turbulent natural convection. He had question about the use of wall function to analyze the turbulent flow by buoyance in enclosure. Nallasamy[9] reviewed the turbulence models and their applications to the prediction of internal flows. He said that the k-ε model is used in majority of all the 2-dimensional flow calculations reported in the literature. So far the laminar natural convection in the inclined enclosure has been studied widely for many engineering applications. Some studies are given by Symons and Peck(1984) and by Goldstein and Wang(1984). But the study on the turbulent natural convection in an inclined enclosure has been rarely presented.

In present study, the phenomena of turbulent natural convection in an inclined square enclosure have been investigated numerically with the k-ε turbulent model. The enclosure is heated differently along the two opposite walls and the other two walls are maintained linear temperature. The hot and cold walls are considered to be isothermal. The inclined angle is zero when the hot and cold walls locate vertically. The inclined angle increases counter-clockwise. To emphasize on the effect of inclined angle, the parameters such as turbulent model, empirical constant, range of the Grashof number, and the Prandtl number are selected same as Fraikin et. al. (1980).

2. MATHEMATICAL FORMULATION AND METHOD OF SOLUTION

2.1 The Governing Equation

The system for present study is depicted schematically in Fig. 1. All fluid properties are treated as constant with the exception of the density appearing in the body force terms. For this term a linear variation of density with temperature is assumed, according to the following equation.

$$\rho=\rho_o\cdot\{1-\beta\cdot(T^*-T_o^*)\} \tag{1}$$

Some simplification of the resulting body force terms is represented by defining an effective pressure, P'.

$$P'=P^*+\rho_o\cdot g\cdot(y^*\cdot\cos\theta+x^*\cdot\sin\theta)+\frac{2}{3}\rho_o\cdot k^* \tag{2}$$

Dimensionless variables are then formed as follows ;

$$T=2\frac{T^*-T_o^*}{T_H^*-T_C^*},\quad x=\frac{x^*}{L/2},\quad y=\frac{y^*}{L/2} \tag{3a}$$

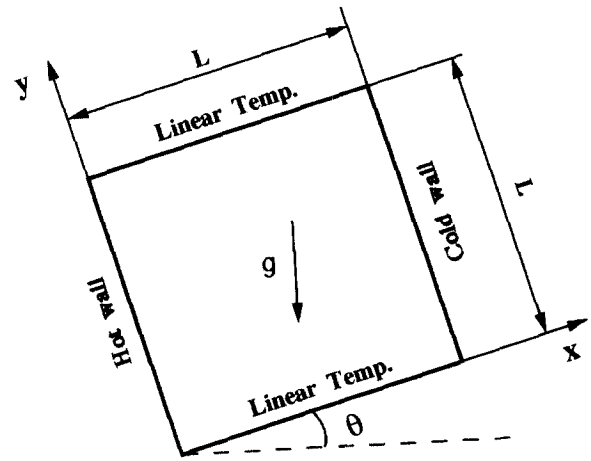

Fig. 1 Schematic representation of inclined square enclosure

$$u=\frac{u^*(L/2)}{\nu},\quad v=\frac{v^*(L/2)}{\nu} \tag{3b}$$

$$k=\frac{k^*(L/2)^2}{\nu^2},\quad \varepsilon=\frac{\varepsilon^*(L/2)^4}{\nu^3},\quad p=\frac{p'(L/2)^2}{\rho_o\cdot\nu^2} \tag{3c}$$

$$\mu_t=\mu_t^*/\mu^*,\quad Gr=g\cdot\beta\cdot(T_H^*-T_C^*)\cdot L^3/\nu^2,\quad Pr=\alpha/\nu \tag{3d}$$

For a steady two-dimensional flow, the following governing equations represent the conservation of the dimensionless time-averaged quantities. The same two-dimensional k-ε model for turbulence as employed by Farouk(1981), Fraikin et al.(1980) and Ozoe et al. (1985) has been used for present study.

$$\frac{\partial u}{\partial x}+\frac{\partial v}{\partial y}=0 \tag{4}$$

$$\frac{\partial}{\partial x}(u^2)+\frac{\partial}{\partial y}(uv)=-\frac{\partial p}{\partial x}+\frac{\partial}{\partial x}\left(\mu_{eff}\frac{\partial u}{\partial x}\right)+\frac{\partial}{\partial y}\left(\mu_{eff}\frac{\partial u}{\partial y}\right)+Su \tag{5}$$

$$\frac{\partial}{\partial x}(uv)+\frac{\partial}{\partial y}(v^2)=-\frac{\partial p}{\partial y}+\frac{\partial}{\partial x}\left(\mu_{eff}\frac{\partial v}{\partial x}\right)+\frac{\partial}{\partial y}\left(\mu_{eff}\frac{\partial v}{\partial y}\right)+Sv \tag{6}$$

$$\frac{\partial}{\partial x}(u\phi)+\frac{\partial}{\partial y}(v\phi)=\frac{\partial}{\partial x}\left(\Gamma_{\phi,eff}\frac{\partial\phi}{\partial x}\right)+\frac{\partial}{\partial y}\left(\Gamma_{\phi,eff}\frac{\partial\phi}{\partial y}\right)+S_\phi \tag{7}$$

Where $\mu_{eff}(=\mu_t+1)$ is the effective viscosity, and Γ_ϕ is the exchange coefficient for the transport of property $\phi(=T, k$ and $\varepsilon)$. The exchange coefficient of energy, turbulent kinetic energy and rate of dissipation of turbulent energy are $\Gamma_{T,eff}=(\mu_t/\sigma_T)+(1/Pr)$, $\Gamma_{k,eff}=(\mu_t/\sigma_k)+1$ and $\Gamma_{\varepsilon,eff}=(\mu_t/\sigma_\varepsilon)+1$, respectively.

The source term, S, in the governing equation are as follows ;

$$Su=\frac{\partial}{\partial x}\left(\mu_t\frac{\partial u}{\partial x}\right)+\frac{\partial}{\partial x}\left(\mu_t\frac{\partial v}{\partial y}\right)+\frac{Gr}{16}\sin\theta\cdot T \tag{8a}$$

$$S_v=\frac{\partial}{\partial y}\left(\mu_t\frac{\partial u}{\partial x}\right)+\frac{\partial}{\partial y}\left(\mu_t\frac{\partial v}{\partial y}\right)+\frac{Gr}{16}\cos\theta\cdot T \tag{8b}$$

$$S_T=0 \tag{8c}$$

Table 1 The constant used in the turubulent modeling

C_μ	C_1	C_2	C_3	σ_k	σ_ε	σ_T
0.09	1.44	1.92	0.7	1.0	1.3	1.0

$$S_k = G - \varepsilon - \frac{Gr}{16}\frac{\mu_t}{\sigma_T}\left(\frac{\partial T}{\partial y}\cos\theta + \frac{\partial T}{\partial x}\sin\theta\right) \tag{8d}$$

$$S_\varepsilon = C_1\frac{\varepsilon}{k}G - C_2\frac{\varepsilon^2}{k} - C_3\frac{\varepsilon}{k}\frac{Gr}{16}\frac{\mu_t}{\sigma_T}\left(\frac{\partial T}{\partial y}\cos\theta + \frac{\partial T}{\partial x}\sin\theta\right) \tag{8e}$$

$$G = \mu_t\cdot\left\{2\left(\frac{\partial u}{\partial x}\right)^2 + 2\left(\frac{\partial v}{\partial y}\right)^2 + \left(\frac{\partial u}{\partial y} + \frac{\partial v}{\partial x}\right)^2\right\} \tag{8f}$$

The turbulent viscosity, μ_t, is related to k and ε as follows;

$$\mu_t = C_\mu\cdot k^2/\varepsilon \tag{9}$$

Rodi(1975) discussed the conditions under which C_μ could be considered constant. Numerical values for C_μ, C_1, C_2, σ_T, σ_k and σ_ε are taken as recommended by Launder and Spalding (1974). The constant C_3 in the buoyancy term of above equation has been adopted from Fraikin et al.(1980). They are given in Table 1.

The following boundary conditions have been used;

$$T=1, \quad u=v=k=0 \ \ at \ \ x=0 \tag{10a}$$

$$T=-1, \quad u=v=k=0 \ \ at \ \ x=2 \tag{10b}$$

$$T=1-x, \quad u=v=k=0 \ \ at \ \ y=0 \text{ and } y=2. \tag{10c}$$

The time-averaged rate of dissipation of turbulent energy, ε, is proportional to $k^{3/2}/l$. Since both k and l approach zero at the wall, the boundary condition for ε is undefined. The ε equation is solved only in a reduced domain excluding the walls. In the present study, the ε value near the wall is fixed same as previous investigators(Fraikin(1980), Markatos and pericleous(1984) and Ozoe et al(1985)), thus

$$\varepsilon_1 = (C_\mu^{3/4}\cdot k_1^{3/2})/(\chi\cdot\Delta_1) \tag{11}$$

where subscript 1 denotes the nearest grid point from the wall. χ is Von Karman's constant having a value of 0.42 and Δ is the dimension of the first node from the wall.

2.2 The Solution Procedure

The governing equations, together with the appropriate boundary conditions, are cast into the finite volume method. The discretization equations are derived by the method of control volume formulation(Patankar 1980). The final discretization equations have a generalized form on a gird point P.

$$a_P\phi_P = \sum a_{nb}\phi_{nb} + b \tag{12}$$

where ϕ denotes u, v, T, k or ε and the subscript nb denotes the neighbor grid point of P. The summation is to be taken over all the neighbors. In the present study, there are four neighbors. The discretization equations are solved by a finite difference calculation procedure called SIMPLE(Semi Implicit Method for Pressure Linked Equation) which is described in detail by Patankar(1981).

A 32×32 grid was employed with a denser nodal point near the walls as shown in Fig. 2. The 42×42 and 52×52 grid were tested for some selected situation. It was found that the grid dependency on the calculated results was within 5% as a whole. In actual computations, almost 800 iterations were needed to get convergent solution. For high Grashof number, the solutions of low Grashof number were used as initial values in the iterative procedure. We believed that the convergence were obtained when the heat balance of the system were agreed within 0.1% and the values of each quantities didn't change within effective four digit during 10 more iterations.

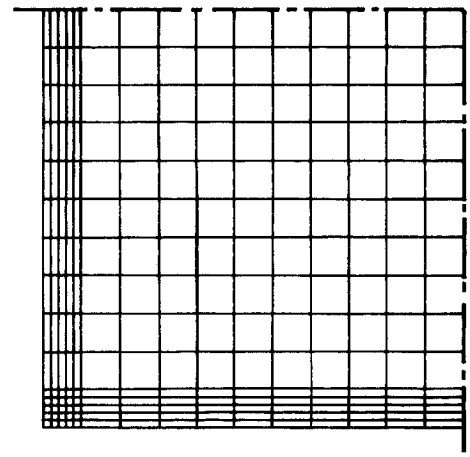

Fig. 2 Grid illustration in the lower left part of the enclosure

3. RESULTS AND DISCUSSION

Numerical solutions were obtained in dimensionless form of velocities, temperature, pressure, stream function, turbulent kinetic energy, rate of dissipation of turbulent energy, turbulent viscosity, local Nusselt number and average Nusselt number. The results are presented for sixteen combinations of the Grashof numbers (6×10^6, 1×10^7, 5×10^7 and 1×10^8) and the inclined angles (0°, 30°, 45° and 60°). To check the validity of present numerical results, at first, solutions at zero inclined angle were compared witht that of Fraikin (1980) as shown in Table 2. Fairly good agreement has been achieved even though the methodology and the gird distribution had been different each other.

3.1 Streamlines

The stream function was obtained from velocity field by evaluating the integral along constant x lines,

Table 2 Comparison of some important quantities between Present and Fraikin et al.(1980) at zero inclined angle

Gr	$\overline{Nu}_H$		$\overline{Nu}_L$		$\mu_{t,max}$	
	Present	Fraikin	Present	Fraikin	Present	Fraikin
6×10^6	12.0	12.2	5.92	6.64	3.73	3.19
10^7	14.3	14.2	6.89	7.53	4.73	4.01
5×10^7	24.1	22.4	11.0	10.6	8.63	7.90
10^8	29.3	26.1	13.0	11.7	9.87	9.58

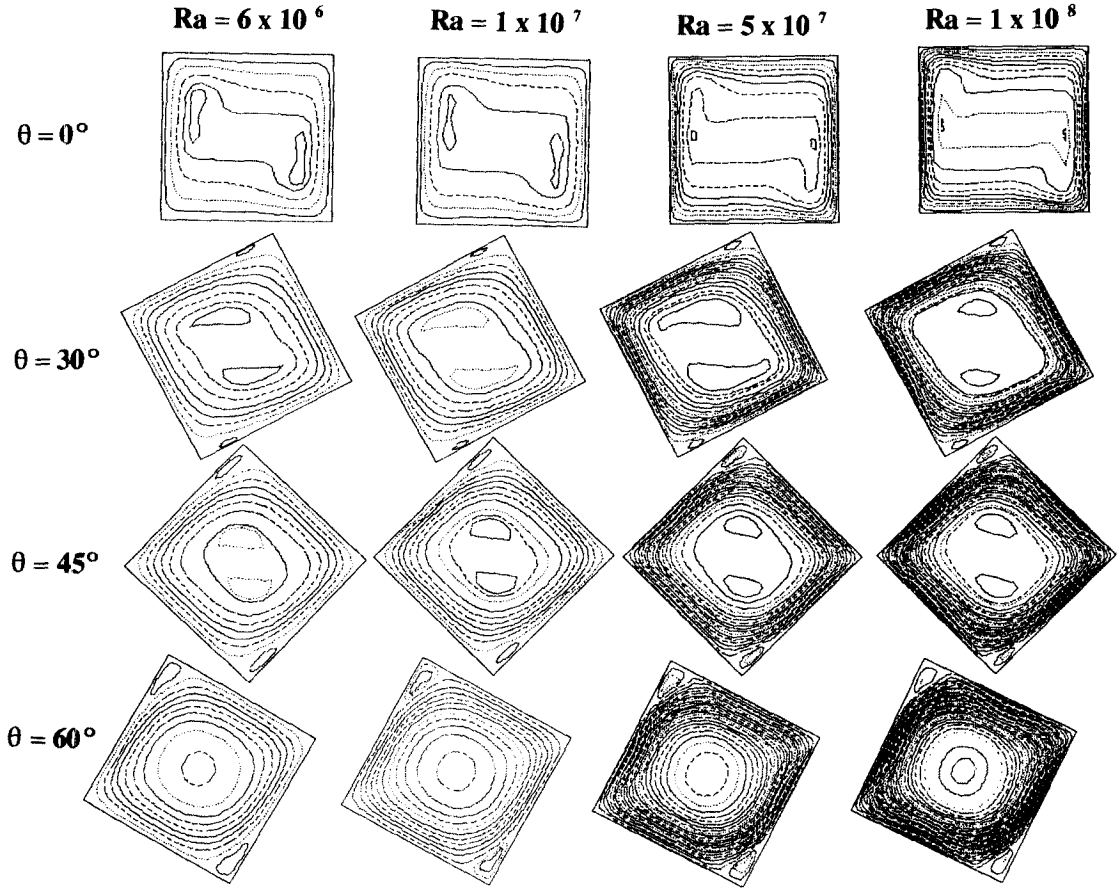

Fig. 3 Numerical Streamlines

$$\varphi = \int_0^y u dy \tag{13}$$

and $\varphi=0$ along the walls. In Fig. 3 sixteen plots of the streamlines which indicate the mean flow pattern are presented. The differences between each neighbor contours are 20 in φ except the central region and the corners where the counter-clockwise flow exists. To show the secondary flow in the core of enclosure, two streamlines of arbitrary value are presented. The effects of inclined angle on the patterns of streamlines are similar each other for all Grashof numbers taken here. When $\theta \leq 45°$, there are the strong clockwise base flow near the wall region and the weak secondary flow in the core region. When $\theta=60°$, this secondary flow disappears so that the strong base flow extends to the core region. The maximum stream function which indicates the intensity of the base flow increases 1.7, 2.0 and 3.0 times as large at the inclined angles of 30°, 45° and 60°, respectively as that of the zero inclined angle. Except zero inclined angle, the counter-clockwise flow occurs in the top and bottom corner. These phenomena are considered as a peculiar influence of the inclined angle. It is believed that this would occur in the inclined enclosure because of the following facts : the hotter fluid started from the hot wall moves up continuously along the inclined top wall of linear temperature. But this upward fluid feels cold near the top corner whose temperature is almost same as that of the cold wall. Therefore, the buoyance force of upward flow decreases so that fluid can not go up anymore. Consequently the fluid near the top corner is isolated and rotates reverse to the base flow. Similar description can be done near the bottom corner.

3.2 Temperature Distribution

Sixteen plots of isotherms are shown in Fig. 4. The dimensionless temperature differences between each isotherm are 0.1. As the Grashof number increases, the temperature gradient becomes high near the wall at all the inclined angles taken here. The influence of inclined angle can be described similarly independent of the Grashof number. At the inclined angle of zero, the horizontal stable stratifications are shown and the range of temperature is large in the core region. As the enclosure exist the angle of inclination, this stratified phenomena disappear, and then the range of temperature becomes small in the core region. Finally at the 60° of the inclined angle, almost zero dimensionless temperatures which indicate the mean value of temperature between the hot and cold walls occupy the core region.

3.3 Turbulent Viscosity

The distribution of dimensionless turbulent viscosity, μ_t, are shown in Fig. 5. The nearest contour at the wall has the value of 1. The values of inner contours are higher by 1 than those of outer contours, so that one can see the maxima near the top corner and the bottom corner. In the core region, the values of contours decrease by 1 toward the center of the

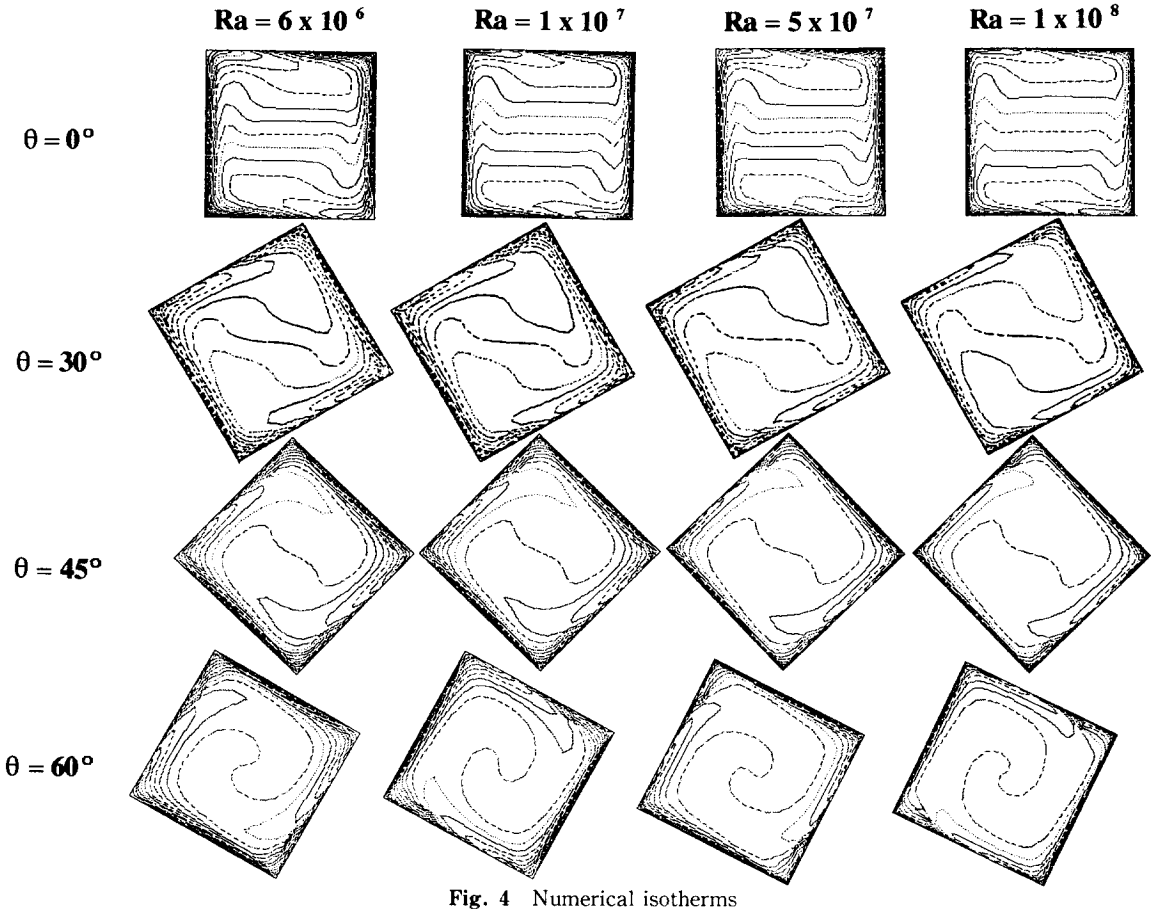

Fig. 4 Numerical isotherms

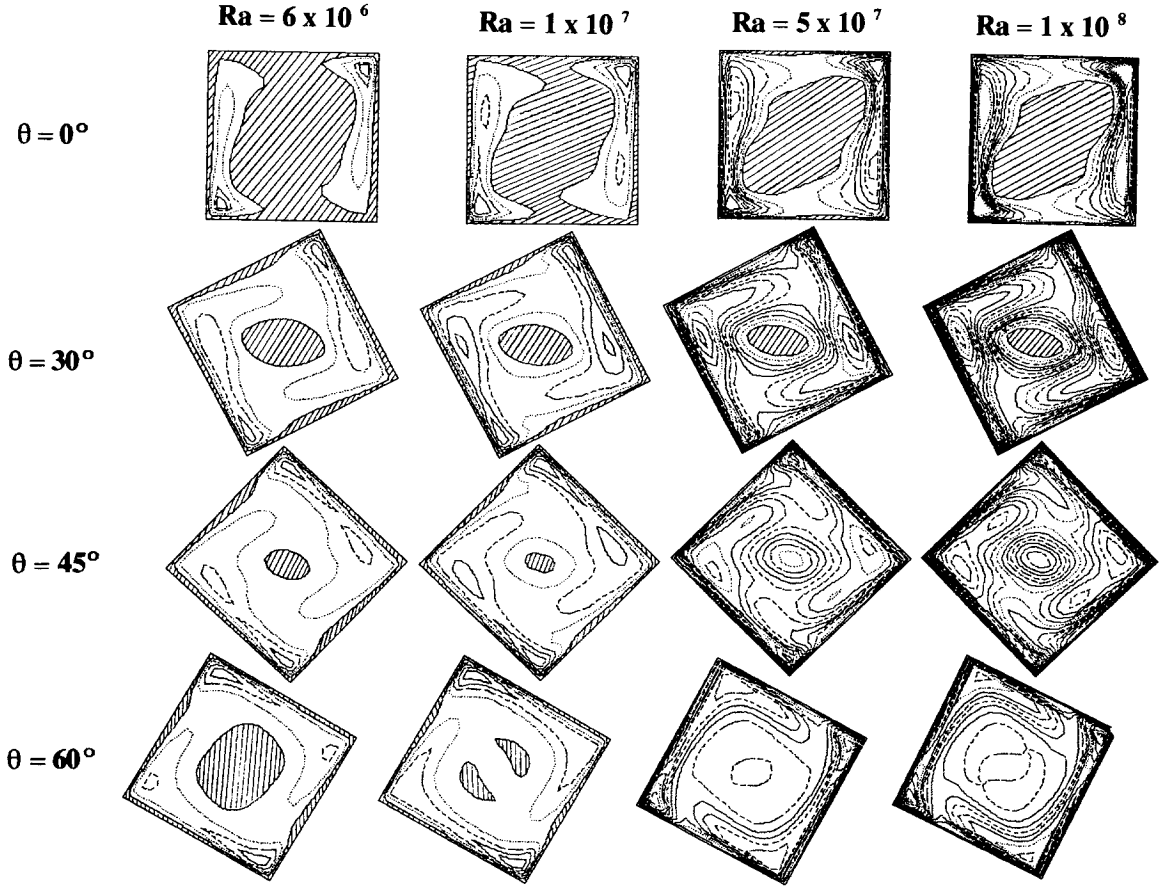

Fig. 5 Numerical contour maps for turbulent viscosity

Table 3 The maximum value of dimensionless turbulent viscosity and the area portion of the significant turbulence in enclosures

θ \ Gr		6×10^6	1×10^7	5×10^7	1×10^8
0°	$\mu_{t,max}$	3.73	4.73	8.62	9.87
	portion(%)	31.4	50.4	55.4	55.4
30°	$\mu_{t,max}$	4.74	5.97	12.4	17.6
	portion(%)	90.1	90.9	95.0	95.0
45°	$\mu_{t,max}$	4.68	5.91	11.6	15.2
	portion(%)	95.0	98.3	100.0	100.0
60°	$\mu_{t,max}$	4.68	5.76	10.2	13.3
	portion(%)	81.0	91.5	100.0	100.0

enclosure. The μ_t indicates the ratio of turbulent visosity to molecular viscosity. Since $\mu_{eff}=\mu_t+1$, in the region where $\mu_t<1$ the molecular viscosity would have priority over turbulent viscosity to determine flow characteristic. Although the flow region where $\mu_t=0$ is laminar one rigorously, the flow region where $\mu_t<1$ could be considered as "quasi-laminar."

In Fig. 5, the region where $\mu_t\leq1$ near the wall and the core of the enclosure are shown by shaded portion. In the region where $\mu_t>1$, the flow can be regarded as a real turbulence or a significant turbulence which has somewhat different meaning from general turbulent flow. According to the inclined angle, the maximum values of turbulent viscosity, $\mu_{t,max}$, and the area portion being occupied by the significant turbulence are listed in Table 3.

The existence of the inclined angle makes the turbulence even strong. For a given Grashof number the $\mu_{t,max}$ occurs at the inclined angle of 30°, while the area portion of the significant turbulence is maximum at the inclined angle of 45°.

It can be seen in Table 3 that, when $Gr\geq5\times10^7$ at the same inclined angle, the $\mu_{t,max}$ is higher with the Grashof number but the area portion of the significant turbulence stays with the Grashof number. Similar results were presented in Fraikin(1980) at the zero inclined angle. When $Gr\geq5\times10^7$ and $\theta\geq45°$, the whole flow region in the enclosures becomes the significant turbulence.

3.4 Turbulent Kinetic Energy

The contours of the dimensionless time-averaged turbulent kinetic energy, k are plotted in Fig. 6. The tendency of distributions of k are much similar to that of μ_t. The differences between two neighbor contours are 2×10^3, 1×10^4 and 2×10^4 for $Gr\leq1\times10^7$, $Gr=5\times10^7$ and $Gr=1\times10^8$, respectively. At the inclined angle of zero, the values of k are high along the hot and cold walls while very low along the walls of linear temperature. As the inlcined angle increases the values of k near the walls of linear temperature become high. This fact could be explained as follows : (1) Since the slope of the walls of linear temperature becomes steeper, the flow can be accelerated. (2) This makes shear stress larger so that the

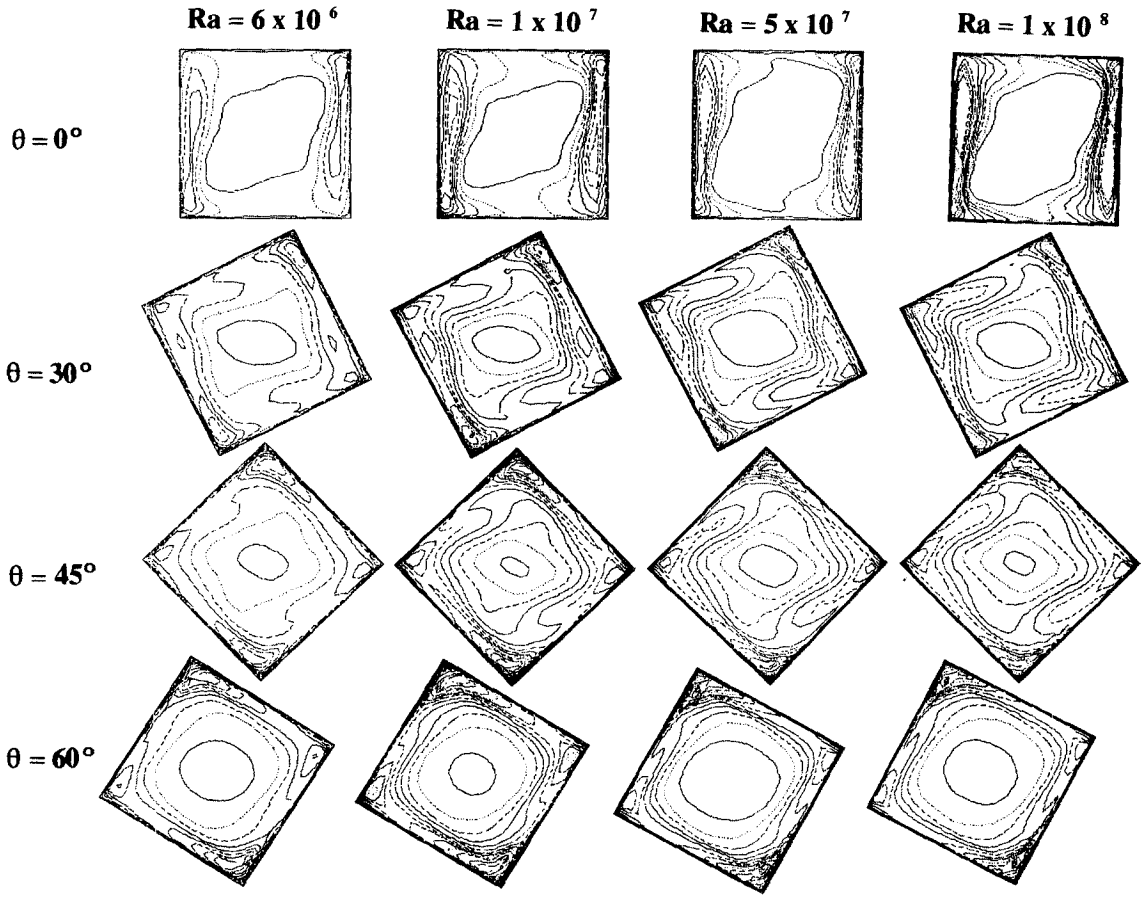

Fig. 6 Numerical contour maps for turbulent kinetic energy

increasing amount of the turbulent kinetic energy, due to shear stress exceeds the decreasing amount of that due to buoyancy. The contours of the rate of dissipation of turbulent kinetic energy, ε, are not presented because its value can be readily obtained from the definition except the region very close to the wall.

3.5 Heat Transfer

The local and average Nusselt numbers along the hot wall are defined as follows;

$$Nu_H = \frac{-(\partial T^*/\partial x^*)_{wall} \cdot L}{(T_H^* - T_C^*)} = -\left.\frac{\partial T}{\partial X}\right|_{wall} \tag{14}$$

$$\overline{Nu_H} = \frac{1}{2}\int_0^2 Nu_H \, dy \tag{15}$$

The Nusselt numbers on the wall of linear temperature, Nu_L and $\overline{Nu_L}$, are defined similarly as along the hot wall. Because of the point symmetric characteristics of present geometry, the Nusselt numbers along the cold wall and the remaining wall of linear temperature do not need to be defined.

Figure.7 and Fig.8 show the distributions of the local Nusselt number along the hot wall and along the wall of linear temperature at each inclined angle when $Gr=10^7$. After continuous investigations about the local Nusselt number at other Grashof number, even though the magnitudes of them are larger with the Grashof number, Fig. 7 and Fig. 8 could be considered as a typical example. On the hot wall (Fig. 7), the location of the maximum local Nusselt number in the inclined enclosures shifts by L/4 toward y-direction as compared with that at the zero inclination. In addition, the values of maximum local Nusselt number increase as the inclined angle increases. On the wall of linear temperature, one can see the peculiar effect of the inclined angle in Fig. 8. Because of the inclined angle, there are one more peak and one more relative minimum at the distributions of the local Nusselt number as compared with that at the zero inclination. Because of inclination, there occurs a reverse flow region with relatively lower velocity near the top and bottom corners as shown in Fig. 3. It is believed that the rate of convective heat transfer becomes small temporally in this reverse flow region.

The average Nusselt number distributions on the hot wall

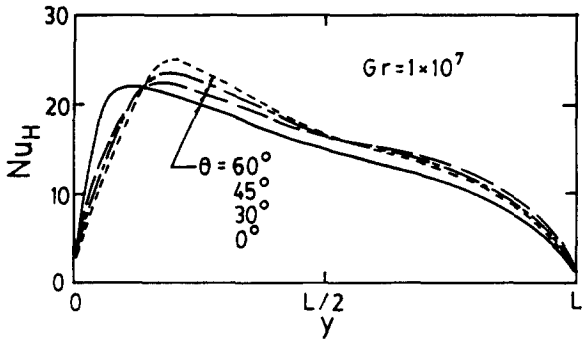

Fig. 7 Distributions of local Nusselt number along the hot wall $Gr=1\times10^7$, $\theta=0°$, 30°, 45° and 60°

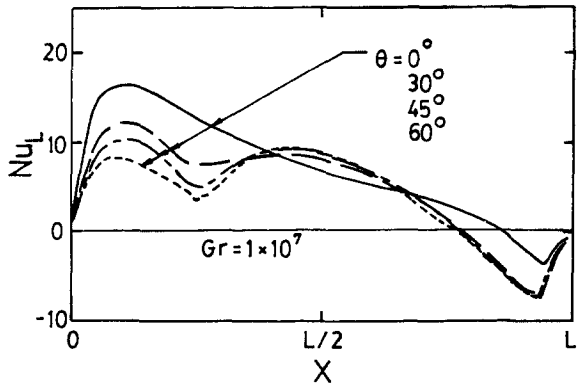

Fig. 8 Distributions of local Nusselt number along the wall of linear temperature
$Gr=1\times10^7$, $\theta=0°$, 30°, 45° and 60°

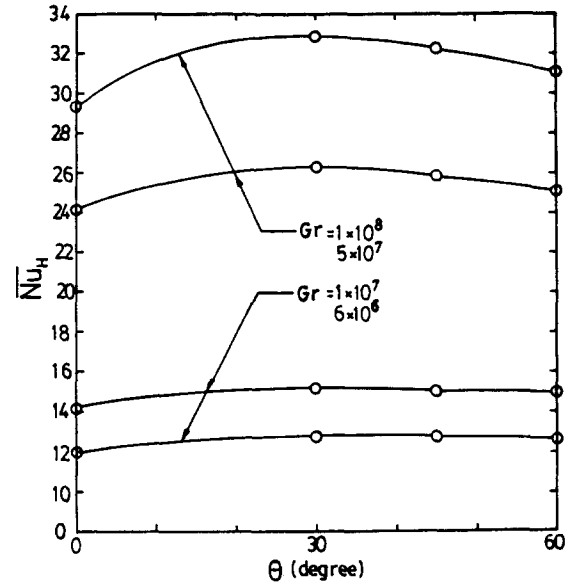

Fig. 9 Effect of inclined angle on $\overline{Nu_H}$ for various Grashof number

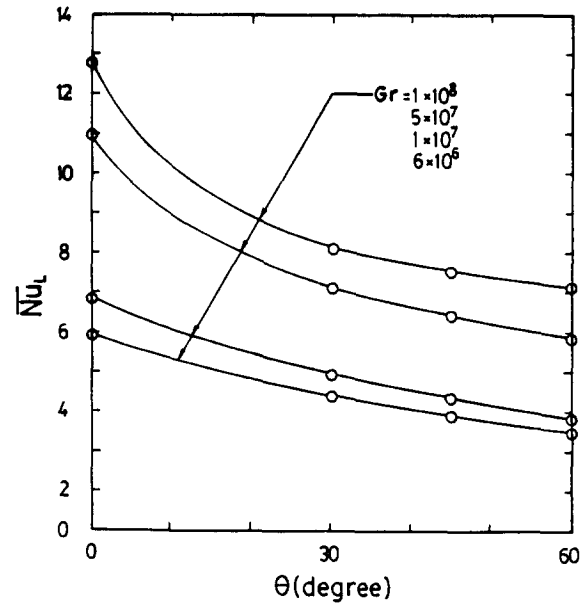

Fig. 10 Effect of inclined angle on $\overline{Nu_L}$ for various Grashof number

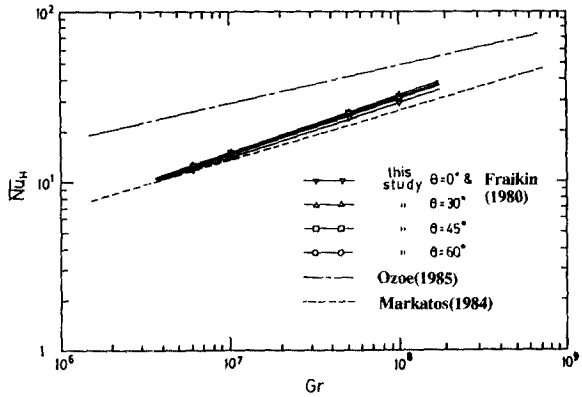

Fig. 11 Comparison of the computed average Nusselt number on the hot wall with correlation of Ozoe(1985), Markatos (1984) and Fraikin(1980)

and the wall of linear temperature are shown in Fig. 9 and Fig. 10, respectively. The $\overline{Nu}_H$ of the inclined enclosure is greater than that at the zero inclination. For example, $\overline{Nu}_H$ has maximum value at $\theta=30^\circ$ which is almost 10% higher than that at $\theta=0^\circ$. But $\overline{Nu}_L$ becomes small as the inclined angle increases. To show the correlation between $\overline{Nu}_H$ and the Grashof number in the inclined enclosure, Fig. 11 is plotted. Although the fluid properties and the boundary conditions were not exactly same, the correlations in the square enclosure of the zero inclination by Ozoe et al.(1985), Makartos et al.(1984) and Fraikin et al.(1980) are plotted together for reference.

4. CONCLUSION

Although the accuracy of the present results should be compared with future experimental work, the application of the k-ε turbulence model to an enclosed buoyancy driven recirculating turbulent flow gives physically reliable results.

From this study, we make the following conclusions:

(1) The existence of the inclined angle

(a) generated the counter-rotating flow region in the enclosure,

(b) made stratification of the temperature field disappear and

(c) made one more peak and one more relative minimum in the distributions of the local heat transfer.

(2) As the inclined angle increased from zero degree,

(a) the intensity of base flow increased and

(b) the area portion in enclosures being occupied by the significant turbulence, where turbulent viscosity is larger than molecular one, became larger.

(3) When $Gr \geq 5\times10^7$ and $\theta \geq 45^\circ$, the whole flow region in the enclosures became the significant turbulence one.

(4) The maximum values of average heat transfer rate on the hot wall was shown at 30° and was almost 10% higher than that at zero degree.

REFERENCES

Davidson, L., 1990(a), "Calculation of the Turbulent Buoyancy-Driven Flow in a Rectangular Cavity Using an Efficient Solver and Two Different Low Reynolds Number k-ε Turbulence Models," Numerical Heat Transfer, Part A, Vol.18, pp.129~147.

Davidson, L., 1990(b), "Second-order Corrections of the k-ε Model to Account for Non-Isotropic Effects due to Buoyancy," Int. Heat and Mass Transfer, Vol.33, No. 12, pp. 2599~2608.

Farouk, B., 1981, Laminar and Turbulent Natural Convection Heat Transfer from Horizontal Cylinders, Ph.D thesis, Univ. of Delaware.

Fraikin, M. P., Portier, J.J. and Fraikin, C.J., 1980, "Application of k-ε Turbulence Model to an Enclosure Buoyance Driven Recirculation Flow," ASME Paper, No.80-HT-68, July pp.1~12.

Goldstein, R. J. and Wang, Q-J., 1984, "An Interferometric Study of the Natural Convection in an Inclined Water Layer," Int. J. Heat Mass Transfer, Vol.27, No.9, pp. 1445~1453.

Ideriah, F.J.K., 1980, "Prediction of Turbulent Cavity Flow Driven by Buoyance and Shear," J. Mech. Engineering Science, Vol.22, No. 6, pp.287~289.

Launder, B.E. and Spalding, D.B., 1974, "The Numerical Computation of Turbulent Flows," Computer Methods in Applied Mechanics and Engineering, 3, pp. 269~289.

Markatos, N.C. and Pericleous, K. A., 1984, "Laminar and Turbulent Natural Convection in an Encloused Cavity," Int. J. Heat Mass Transfer, Vol.27, No.5, pp.755~772.

Nallasamy, M., 1987, "Turbulence Models and their Applications to the Prediction of internal Flows : A Review," Computers & Fluids, Vol.15, No.2, pp.151~194.

Ozoe, H., Mouri, A., Ohmuro, M., Churchill, S.W. and Lior, N., 1985, "Numerical Calculations of Laminar and Turbulent Natural Convection in Water in Rectangular Channels Heated and Cooled Isothermally on the Opposing Vertical Walls," Int. J. Heat Mass Transfer, Vol.28, No. 1, pp. 125~138.

Patankar, S.V., 1980, Numerical Heat Transfer and Fluid Flow, Mc-Graw Hill Publishing Company, New York.

Patankar, S.V., 1981, "A Calculation Procedure for Two-dimensional Elliptic Situation," Numerical Heat Transfer, Vol.4, pp.409~425.

Rodi, W., 1975, "A Note on the Empirical Constant in the Kolmogorov-Prandtl Eddy-Viscosity Expression," J. of Fluid Eng., ASME, Vol.97, Sept. pp.386~389.

Symons, J.G. and Peck, M.K., 1984, "Natural Convection Heat Transfer through Inclined Longitudinal Slots," J. of Heat Transfer, ASME, Vol.106, Nov., pp.824~829.